Numerical study of steady flow inside a lid-driven square cavity for Reynolds number up to 50000

Azzouz Amin[a], Houat Samir[b], Benhizia Oussama[c]

a. Institut de Maintenance et de Sécurité Industrielle, IMSI, Université d'Oran, Oran, Algéria,
E-mail: aminazouz31@yahoo.com
b. Laboratoire de modélisation numérique et expérimentale de phénomènes mécaniques, MNEPM, Université de Mostaganem, Mostaganem, Algéria
E-mail: sa_houat@yahoo.fr
c. Institut de Maintenance et de Sécurité Industrielle, IMSI, Université d'Oran, Oran, Algéria,
E-mail: benhizia_oussama@yahoo.fr

Abstract :

The flow inside a lid-driven square cavity has been imposed a wide controversy during these last decades. Several studies found to exist in the literature included this case, which is widely used for benchmarking in computational fluid dynamic due to the simplicity of geometry. Some classes of studies have investigated the existence of steady flow in the driven cavity, they found a steady 2D numérical solution until 35000 value of Reynolds number. However, other classes of studies have stated that the flow in driven cavity submitted to a hydrodynamic instability and they illustrated a continuation méthode to locate the point at which a Hopf bifurcation occurs leading to a transition from a steady flow to unsteady. In the shade of these studies and with this uncertainty that surrounded this subject we wanted to get more clarification especially for steady flow solutions. The present study represents a numerical computation for steady flow inside a lid-driven square cavity, the governing equation is solved using a finite volume method based on second order scheme of accuracy. Steady solutions are obtained for Reynolds numbers ascending from 100 to 50000, using a resolution of 1024 x1024 grid point. A good agreement with the previous results in the literature, the work was done in this paper including proprieties of flow in the center of primary and secondary vortices, velocity components and numérical values for stream function and vorticity which assure a good example for benchmarking purposes.

Keywords : lid-driven cavity, steady solutions, finite volume method

1 Introduction

The classical problem of the lid-driven cavity has been an interesting subject for many decades in the domain of computational fluid dynamics, and with a progress of the numerical methods applied this problem has been studied extensively by numerous authors through several studies. In order to prove the effectiveness of the numerical methods and get more accurate results.

Multiple works have been reported in the literature which can be divided into two main sections of studies. Works that are included in the first section represent steady solutions at various Reynolds numbers ranging from low numbers and even at very high Reynolds numbers. In order to investigate the possibility of computation of steady state flow in the lid -driven cavity at these limits, starting first with the numerical and analytical work of Burggraf [1]. Botella et Peyret [2] have investigated the effectiveness of Chebyshev collocation method for highly-accurate solutions at Re=1000 as well as Carlos Henrique Marchi et al [3] based on the finite volume method to get high accurate steady results for Re ≤ 1000. Moreover, Vanka[4] have presented steady solution does not exceed Re=5000 using a

method that solves the Navier-Stocks equations in primitive variables based on a coupled block-implicit multigrid procedure. Recently, AbdelMigid et al [5] have solved the governing equation by GPU accelerated code in which the Finite Volume Method (FVM) in primitive variable formulation was used, they have investigated steady solutions of flow for $Re \leq 5000$.
Bruneau et Jourou [6] have illustrated the efficiency of the multigrid method by solving the Navier-Stocks equations in primitive variable, based on the coupled scheme with a simplified (FMG-FAS) algorithm and a cell by cell relaxation procedure which is very stable, steady solutions was computed up to Re=5000 in which solutions for Re=7500 become unstable. Hou et Zou [7] have demonstrated the capabilities and the efficiency of the lattice Boltzmann method in which steady solutions have computed for $Re \leq 7500$. Zhang [8] relied on the fourth-order compact discretization formule which used in conjunction with multigrid techniques to simulate the flow in steady state for solutions up to Re=7500. the well-known, Ghia et al [9] have used the coupled strongly implicit multigrid (CSI-MG) to study its effectiveness and succeed to get steady solutions for $Re \leq 10000$.Schreiber et Keller [10] have obtained a steady viscous incompressible flow for $Re \leq 10000$ by the efficient and the reliable numerical techniques based on a combination of a linear system solver, an adaptive newton -like method for nonlinear system and a continuation procedure for following a branch of solutions over a range of Reynolds numbers. Gupta et Kalita [11] have tested the biconjugate gradient method to obtain steady numerical solutions for $Re \leq 10000$, they found a high accuracy with results available in the literature. Barragy et Carey [12] based on the p-type finite element scheme, steady solutions was provided up to Re=12500 while Erturk et al [13] are example of steady solutions for $Re \leq 21000$ using a very efficient finite difference (fourth-order compact formulation) and a very fine grid mesh with a maximum absolute residuals that were less than 10^{-10}, They stated that a fine grid mesh is necessary in order to obtain a steady solutions and allowed to resolve the vortices appear in the corners. followed by the work of Erturk [14] which basically discusses in details the flow in driven cavity physically, mathematically and numerically, a very fine grid mesh was used in order to get steady solutions results for $Re \leq 20000$. A discussion of the exhaustive use and implementation of stabilization finite element methods was presented by Hachem et al [15] for the resolution of 3D time-dependent incompressible flow. in the same way, 2D incompressible flow in driven-cavity was computed until Re=20000. however, solutions for Re=33000 and Re=50000 were unstable. A compact fourth-order-accurate central difference scheme was used to discretize the stream function -vorticity formulation illustrated by Wahba [16] and succeed to get steady and stable solutions even Re=35000.Additionally, the adoption of the line implicit time marching scheme is to enhance numerical stability and to allow the control of the convergence rates.

On the other hand, in the second section of studies, authors have been shown that flow inside a lid-driven cavity is not steady at hight Reynolds numbers, and they stated that there exist a Hopf bifurcation due to a hydrodynamical instability in which a transition from steady state to unsteady state happened, various results were reported and disagree in where the first Hopf bifurcation occurs. Peng et al [17] carried out a direct numerical simulation method basically about the transition process from laminar to chaotic flow, they have located the first Hopf bifurcation under Re=7500. Auteri et al [18] have presented a numerical investigation by applying a second-order spectral projection method and solving the unsteady Navier-Stokes equations in primitive variables, their results show that the first Hopf bifurcation is in the interval $8017.6 \leq Re \leq 8018.8$.
Fortin et al [19], Sahin et Owens [20], Abouhamza et Pierre [21] and Gervais et al [22] gave it close to Re=8000. Notably, their studies focused on the hydrodynamical stability analysis. Bruneau and Saad[23] relied on a finite differences discretization where a multigrid solver combined with relaxation procedure with a cell by cell. furthermore, in to achieve more stability a new third order scheme is constructed for the convective term, they have obtained the first Hopf bifurcation at Re=8000, however, a mainly periodic solution was described at Re=10000. It is obvious that the Hopf

bifurcation in the range of 7500 ≤ Re ≤ 10000 from the content of the above studies, even though there exist other work in the literature reported that it may be found even close to Re=30000.

From the previously mentioned studies and another present in the literature, it turns out that the steady solution flow in the lid-driven cavity was carried out for highest Reynolds number equal to Re=35000. Although there are other results for higher Reynolds numbers except that are not steady. for that reason, the present study aimed to investigate the possibility of computation of steady two dimentional incompressible flow in square lid driven cavity even on a very high Reynolds numbers, ranging for a wide fields starting from 100 up to 50000, and to verify the effectiveness of the Finit Volume Method (FVM) based on the second order scheme of accuracy where a very fine grid of 1024×1024 was used.Table 1 summarizes the main features for references reported in the literature for the highest Reynolds numbers with stable solutions.

Table1: Method's applied Reynolds number and grid formulation for classical problem. FDM: finite difference method, FVM : finite volume method, FEM : finite element method, LB: lattice boltzmann method, Cheb : Chebyshev collocation,cG: continuous Galerkin.

Authors	Re	Method	Formulation	Grid
(1982)-Ghia et al[9]	100-10000	FDM	ψ-ω	129×129-256×256
(1983)-Schreiber Keller[10]	1-10000	FDM	ψ-ω	121×121 -180×180
(1986)-Vanka[4]	100-5000	FDM	ψ-ω	41×41 - 321×321
(1990)-Bruneau et Jourou[6]	100-15000	FDM	u, v, p	64×64-256×256
(1995)-Hou et Zou [7]	100-7500	LB	BGKmodel	256×256
(1997)-Barragy et Carey[12]	1E-04-10000	FEM	ψ-ω	257×257
(1998)-Botella et peyret[[2]	100-1000	Cheb	u, v, p	160
(2003)-Zhang [8]	100-7500	FDM	ψ-ω	17×17-129×129
(2005)-Gupta et Kalita[11]	100-10000	FDM	ψ-V	41×41-161×161
(2005)-Erturk et al[13]	1000-21000	FDM	ψ-ω	601×601
(2008)-Carlos Henrique Marchi et al[3]	100-1000	FVM	u, v, p	2×2-1024×1024
(2009)-Erturk [14]	1000-20000	FDM	ψ-ω	257×257-1025×1025
(2010)-Hachem et al[15]	20000	cG-FEM	u, v, p	180×180
(2012)-Wahba[16]	1000-35000	FDM	ψ-ω	127×127-501×501
(2016)-AbdelMigid et al [5]	100-5000	FVM	u, v, p	601×601-1301×1301

2 Mathematical model and numerical method

2 1 Mathematical model

Fundamentally the mathematical model considered based on the conservation equation laws (N.S.equations). Equations of conservation of mass and momentum (1) to (3) will be simplify considering a two-dimensional, laminar, incompressible, Newtonian fluid flow on steady state in square lid driven cavity as folow:

$$\frac{\partial u}{\partial x} + \frac{\partial v}{\partial y} = 0 \qquad (1)$$

$$\rho \frac{\partial (u^2)}{\partial x} + \rho \frac{\partial (uv)}{\partial y} = \mu \left(\frac{\partial^2 u}{\partial x^2} + \frac{\partial^2 u}{\partial y^2} \right) - \frac{\partial p}{\partial x} \qquad (2)$$

$$\rho \frac{\partial (uv)}{\partial x} + \rho \frac{\partial (v^2)}{\partial y} = \mu \left(\frac{\partial^2 v}{\partial x^2} + \frac{\partial^2 v}{\partial y^2} \right) - \frac{\partial p}{\partial y} \qquad (3)$$

Where p represent the pressure, u and v are velocity components on x and y coordinate, respectively, μ is the dynamic viscosity, ρ expresses the fluid density.

The Reynolds number is defined as :

$$Re = \frac{\rho V L}{\mu} \qquad (4)$$

Where V is the velocity vector, L signifies the length (physical size of the cavity).

The formulations that relate the stream -function to velocity components can be written as follow:

$$u = \frac{\partial \psi}{\partial y} \quad , v = -\frac{\partial \psi}{\partial x} \qquad (5)$$

Where ψ represents the stream function.

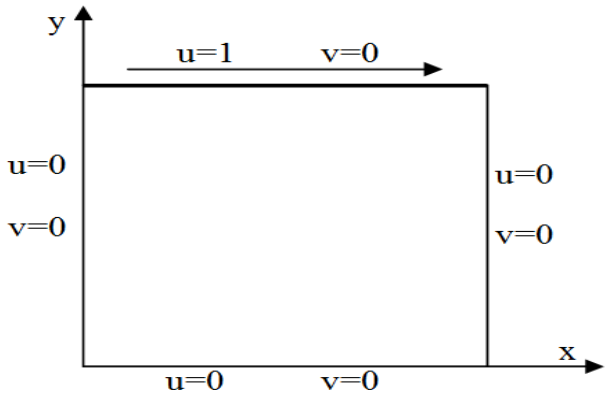

Figure 1 Boundary conditions for clasical problem.

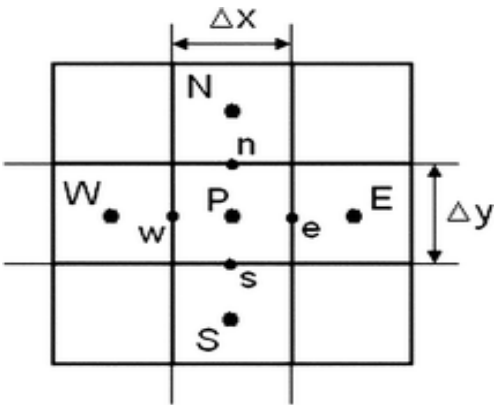

Figure 2 Control volume in 2D.

2 2 Numerical method
Method applied

In order to to solve the mathematical model described by conservation equations (1) to (3), We rely on the finit volume method (FVM) based on a second order scheme. Briefly, the method uses the integral form of the conservation equations as a starting point. The domain of calculation is subdivided into a finite number of contiguous control volumes (CV) in which the conservation equations are applied to each control volume (CV), see Ferziger et Peric[24]. The variable values at the centroid of each control volume(CV) will be calculated. Additionally, in order to convert the general differential equation into a system of algebraic equation for each control volume (CV) an approximation method is used for each surface and volume integral.

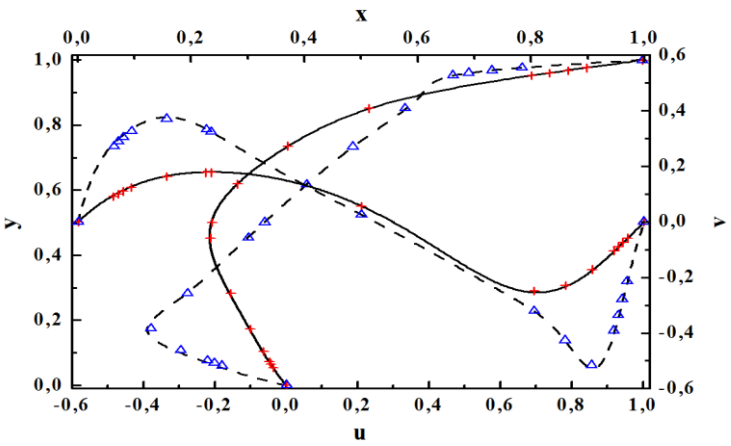

Figure 3 Comparison of u-velocity on the vertical centerline at (x=0.5) and v-velocity on the horizontal centerline at (y=0.5): full lines represent Re=100 for present study, Δ represent Ghia et al [9] result at Re=100, dashed lines represent Re=1000 for present study, + represent Ghia et al [9] result at Re=1000.

2 3 Relaxation Scheme

Solving the flow in a coupled manner ,by meaning that the momentum equations (2,3) and the continuity equation (1) were solving together, allow the use of an implicit relaxation where a under-relaxation factor is used in correlation with the flow courant number (CFL) enables the control of stability and the convergence behavior.

Table 2 Comparison with previous results the location of primary and secondary vortices for diferent Reynolds numbers.

Re	Author	Primary Vortex		Right secondary vortex		Left secondary vortex	
		x	y	x	y	x	y
100	Ghia et al [9]	0.6172	0.7344	0.9453	0.0625	0.0313	0.0391
	Vanka [4]	0.6188	0.7375	0.9375	0.0563	0.0375	0.0313
	Schreiber et Keller [10]	0.6167	0.7417	0.9417	0.0500	0.0333	0.0250
	Hou et Zou [7]	0.6196	0.7373	0.9451	0.0627	0.0392	0.0353
	Bruneau et Jouron [6]	0.6172	0.7344	0.9453	0.0625	0.0313	0.0391
	Zhang [8]	0.6172	0.7343	-	-	-	-
	Ghupta et Kalita [11]	0.6125	0.7375	0.9375	0.0625	0.0375	0.0375
	Carlos Henrique Marchi et al [3]	0.6162	0.7373	-	-	-	-
	AbdelMigid et al [5]	0.6156	0.7371	0.9418	0.0616	0.0333	0.0349
	Present	**0.6157**	**0.7373**	**0.9424**	**0.0618**	**0.0345**	**0.0344**
400	Ghia et al [9]	0.5547	0.6055	0.8906	0.1205	0.0508	0.0469
	Vanka [4]	0.5563	0.6000	0.8875	0.1188	0.0500	0.0500
	Schreiber et Keller [10]	0.5571	0.6071	0.8857	0.1143	0.0500	0.0429
	Hou et Zou [7]	0.5608	0.6078	0.8902	0.1255	0.0549	0.0510
	Ghupta et Kalita [11]	0.5563	0.6000	0.8875	0.1188	0.0500	0.0500
	Carlos Henrique Marchi et al [3]	0.5537	0.6054	-	-	-	-
	AbdelMigid et al [5]	0.5541	0.6057	0.8852	0.1215	0.0516	0.0466
	Present	**0.5541**	**0.6055**	**0.8853**	**0.1224**	**0.0512**	**0.0471**
1000	Ghia et al [9]	0.5313	0.5625	0.8594	0.1094	0.0859	0.0781
	Vanka [4]	0.5438	0.5625	0.8625	0.1063	0.0750	0.0813
	Schreiber et Keller [10]	0.5286	0.5643	0.8643	0.1071	0.0857	0.0714
	Hou et Zou [7]	0.5333	0.5647	0.8667	0.1137	0.0902	0.0784
	Bruneau et Jourou [6]	0.5313	0.5586	0.8711	0.1094	0.0859	0.0820
	Zhang [8]	0.5313	0.5625	-	-	-	-
	Ghupta et Kalita [11]	0.5250	0.5625	0.8625	0.1063	0.0750	0.0813
	Carlos Henrique Marchi et al [3]	0.5312	0.5654	-	-	-	-
	Botella et Peyret [2]	0.5308	0.5652	0.8711	0.1094	0.0859	0.0820
	Ercan Erturk [14]	0.5313	0.5654	0.8643	0.1123	0.0830	0.0781
	AbdelMigid et al [5]	0.5308	0.5657	0.8636	0.1115	0.0832	0.0782
	Present	**0.5308**	**0.5653**	**0.8640**	**0.1117**	**0.0832**	**0.0780**
3200	Ghia et al [9]	0.5165	0.5469	0.8125	0.0859	0.0859	0.1094
	Zhang [8]	0.5157	0.5390	-	-	-	-
	Ghupta et Kalita [11]	0.5188	0.5438	0.8125	0.0875	0.0813	0.1188
	AbdelMigid et al [5]	0.5175	0.5408	0.8236	0.0849	0.08153	0.1198
	Present	**0.5178**	**0.5404**	**0.8236**	**0.0841**	**0.0811**	**0.1199**

Additionally, the coupled approach offers some advantages over the non-coupled or segregated approach represented in a robust and efficient phase implementation. because of the use of a high

Reynolds numbers for a steady state in this study, a main problem of instability is posed, due to high-frequency errors which affect the results and here it illustrates the effectiveness of the relaxation scheme , the flow courant number (CFL) is ranging from CFL=20 for high Reynolds numbers up to CFL=200 for low Reynolds numbers. Otherwise, the under-relaxation factor (α) is ranged from α=0.35 for high Reynolds numbers to α=1 for lower Reynolds numbers, a large number of flow courant numbers leads to fast convergence, whereas a low number leads to a slower convergence and an enhancement on the stability of the convergence behavior.

Table 3 Comparison of stream function and vorticity value for primary and secondary vortices for different Reynolds numbers with previous results.

Re	Authors	Primary vortex		Right Secondary vortex		left secondary vortex	
		ψ	ω	ψ	ω	ψ	ω
100	Ghia et al [9]	-0.103423	3.16646	1.25374E-05	-3.30749E-02	1.74877E-06	-1.55509E-02
	Vanka [4]	0.1034	-	-1.14E-06	-	-1.94E-06	-
	Schreiber et keller [10]	-0.10330	-3.18200	1.320E-05	2.550E-02	2.05E-06	7.9800E-02
	Hou et Zou [7]	0.1030	3.1348	-1.22E-05	-	-1.72E-06	-
	Zhang [8]	0.103511	3.168745	-	-	-	-
	Gupta et Kalita [11]	-0.103	-	1.45E-05	-	1.83E-06	-
	AbdelMigid et al [5]	-0.103516	3.156202	1.3E-05	-3.5775E-02	1.80683E-06	- 1.340214E-02
	Present	**-0.1035204**	**-3.16698**	**1.274E-05**	**3.524367E-02**	**1.81E-06**	**1.50452E-02**
1000	Ghia et al [9]	-0. 117929	2.04968	1.75102E-03	-1.15465	2.31129E-04	-0.36175
	Schreiber et keller [10]	-0.11603	-2.02600	1.700E-03	0.9990	2.1700E-04	0.30200
	Botella et Peyret [2]	0.1189366	2.067753	-1.72717E-03	-1.109789	-2.33453E-04	-0.3522861
	Ercan Erturk [14]	-0.118888	2.067052	1.7287E-03	1.111550	2.3314E-04	0.350476
	Wahba [16]	-0.11894	-2.0677	-	-	-	-
	AbdelMigid et al [5]	-0.118866	2.066581	1.732E-03	-1.113969	2.33412E-04	-0.3409262
	Present	**-0.118929**	**-2.0676**	**1.73030E-03**	**1.107643**	**2.33412E-04**	**0.351918**
5000	Ghia et al [9]	-0.118966	1.86016	3.08358E-03	-2.66354	1.36119E-03	-1.53055
	Vanka [4]	0.0920	-	-5.49E-03	-	-1.67E-03	-
	Ercan Erturk [14]	-0.121942	-1.936291	3.0677E-03	2.720926	1.3729E-03	1.510725
	Wahba [16]	-0.1222	-1.9403	-	-	-	-
	AbdelMigid et al [5]	-0.122069	-1.938057	3.078E-03	-2.750446	1.375483E-03	-1.494181
	Present	**-0.122185**	**-1.940286**	**3.07433E-03**	**2.751347**	**1.374882E-03**	**1.518596**
10000	Ghia et al [9]	-0.119731	1.88082	3.41831E-03	-4.0531	1.51829E-03	-2.08560
	Schreiber et keller [10]	-0.10284	-1.62200	2.96E-03	3.031	-	-
	Gupta et Kalita [11]	-0.122	-	3.22E-03	-	1.50E-03	-
	Ercan Erturk [14]	-0.121781	-1.909677	3.1846E-03	3.751749	1.6118E-03	2.145982
	Wahba [16]	-0.122	-1.9171	-	-	-	-
	Present	**-0.122323**	**-1.91861**	**3.1888E-03**	**3.781775**	**1.6149E-03**	**2.149298**
15000	Ercan Erturk [14]	-0.121342	-1.895353	2.9991E-03	4.938041	1.6730E-03	2.507351
	Wahba [16]	-0.1218	-1.9052	-	-	-	-
	Present	**-0.1221**	**-1.9090**	**2.9993E-03**	**4.9992**	**1.6753E-03**	**2.5256**
20000	Ercan Erturk [14]	-0.120865	-1.884630	2.8038E-03	6.080160	1.6298E-03	2.932753
	Wahba [16]	-0.1213	-1.8974	-	-	-	-
	Present	**-0.12202**	**-1.903689**	**2.79857E-03**	**6.216516**	**1.63011 E-03**	**2.957627**

3 Results and discussions

Flow is driven by the top lid of the cavity with different velocity values while the three remaining walls are in stationary state as shown in Fig 1. in order to access results on an extended field of Reynolds numbers, values of density ρ and dynamic viscosity μ has been regularized in a way that facilitates the computation for all Reynolds numbers. while the convergence criteria adopted in this paper was based on a maximum residual of RES= 10^{-9} for both momentum and continuity equations as a measure of confirmation the convergence to the steady state with very accurate solutions. for all the results presented below, a very fine uniform grid mesh with a resolution of 1024×1024 as Erturk [9] was used.

Fig 2 describes a control volume in Two dimensions (2D) with cell faces E , S, W, N. in which are approximated by the midpoint rule in terms of the nodal P (control volume center), Ferziger et Peric[24].

for the sake of verifying the accuracy of the numerical code represents herein a wide validation of numerical solutions has been done by comparing with previous results which are considered a reference in driven cavity subject. At first, Fig 3 presents u,v velocity profiles through the vertical and the horizontal centerline respectively for both Re=100,1000 Reynolds numbers comparing with results of Ghia et al [9] computed for 129×129 grid mesh, a good correlation between the two results. Additionally Table 2 includes the location of primary and the two first secondary vortices at the bottom of the cavity for $100 \leq Re \leq 3200$ in comparison with large numbers of studies reported above [2,3,4,5,6,7,8,9,10,11]. While values of stream function and vorticity for $100 \leq Re \leq 20000$ tabulated in Table 3 show a very good accuracy especially with [2,5,7,9,14,16], where the significant difference value of stream function from these reference varies less than 0.85% from the present work for Re=1000 in the primary vortex and 0.98% for the other two remaining secondary vortices.as well as,

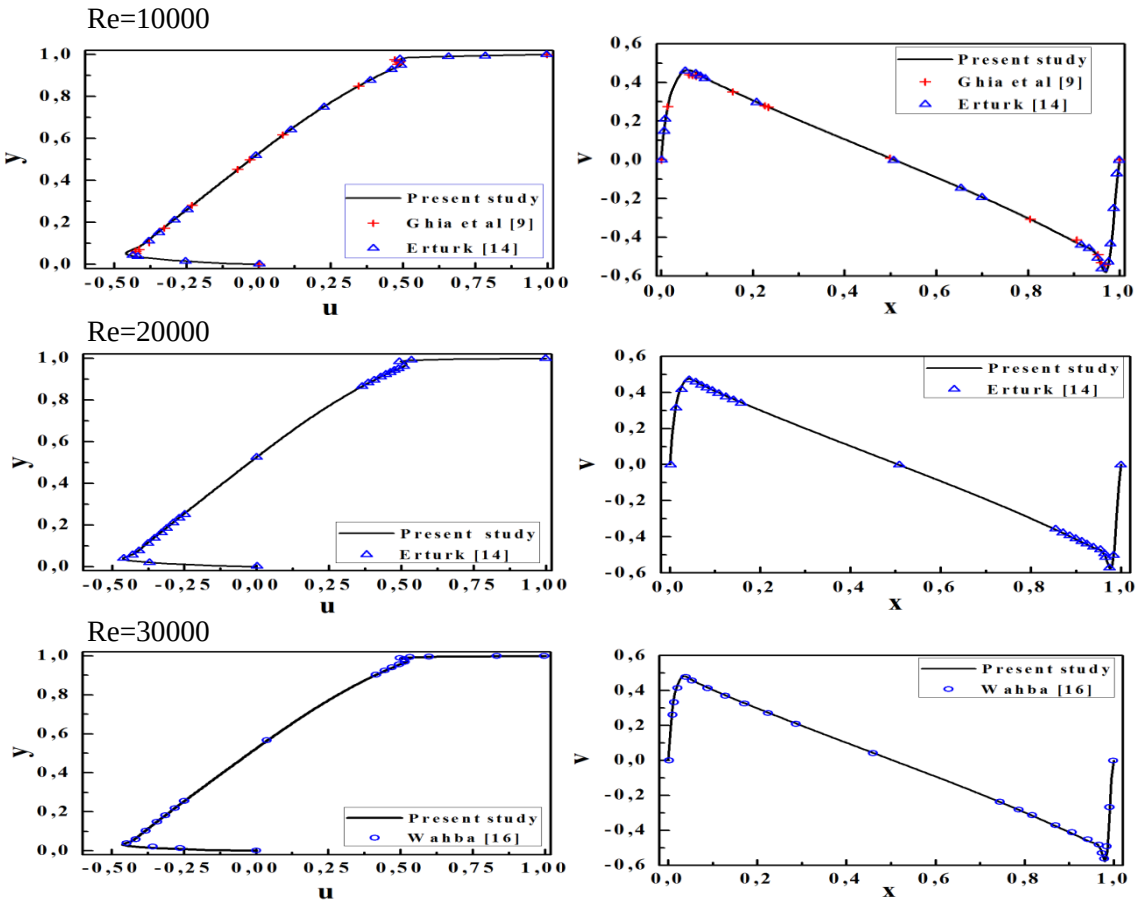

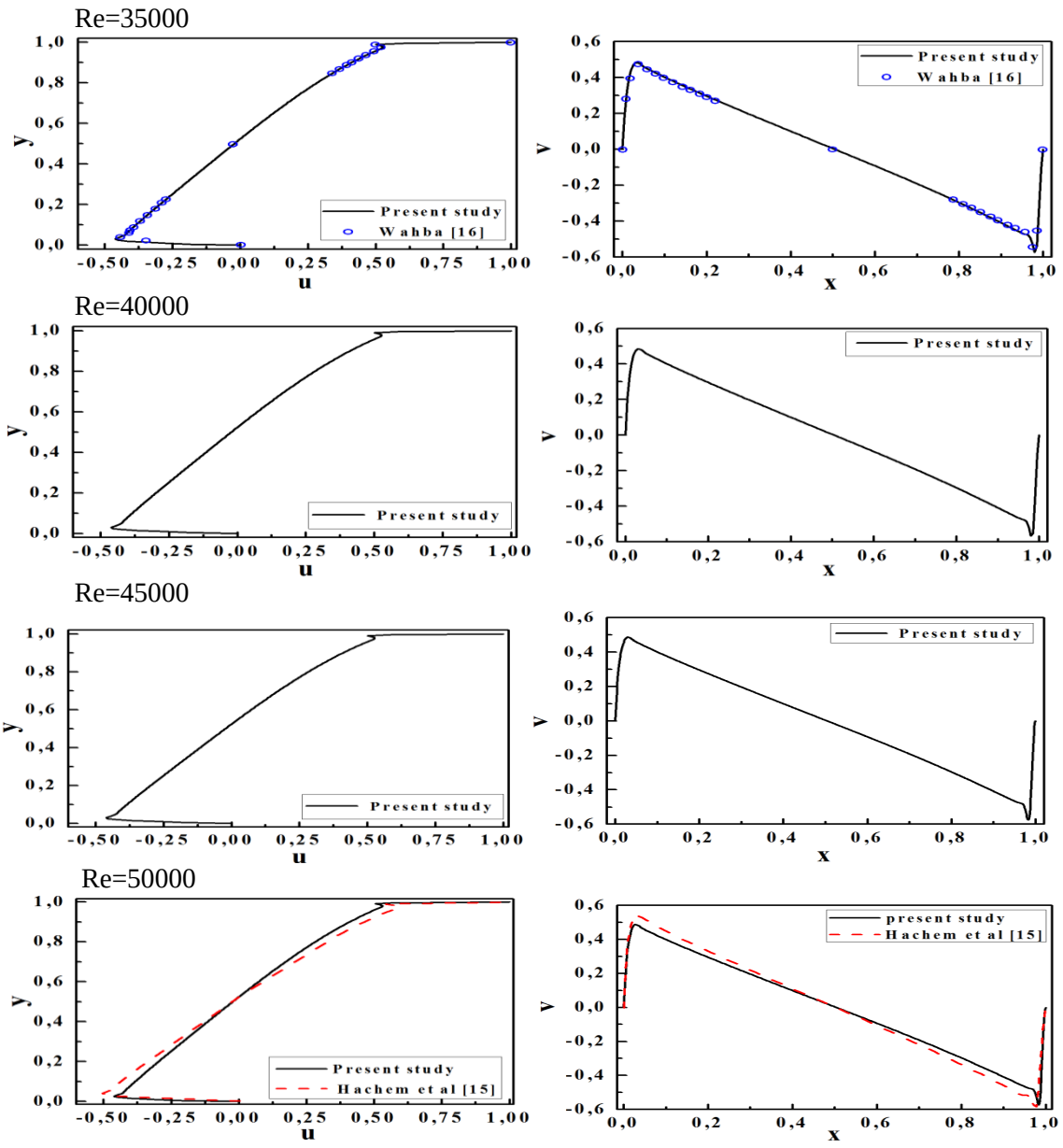

Figure 4 left graphs: u-velocity profiles along the vertical centerline at x=0.5,right graphs:v-velocity profiles along the horizontal centerline at y=0.5.

the vorticity for a maximum difference of 0.87% for the primary vortex and 4.07% for the two secondary vortices, knowing that it was observed a significant numerical approach of the current work with the recently done by AbdelMigid et al [5] It should be noted that it is difficult to reach steady solutions at high Reynolds numbers, Erturk [14] declared that when we increase the grid points to a very fine resolution allows obtaining steady solutions .furthermore, studies which have been reported that the flow in lid-driven cavity subjected to a Hopf bifurcation leading to the appearance of periodic numerical solution because of the coarse grid mesh , also if a sufficiently fine grid mesh used these results would achieve stable solutions even at very high Reynolds numbers. Depending on that, the effectiveness of the present numerical code and the coupling between the momentum equations (2,3) and the continuity equation (1) supported to a very fine grid mesh used in the present study have

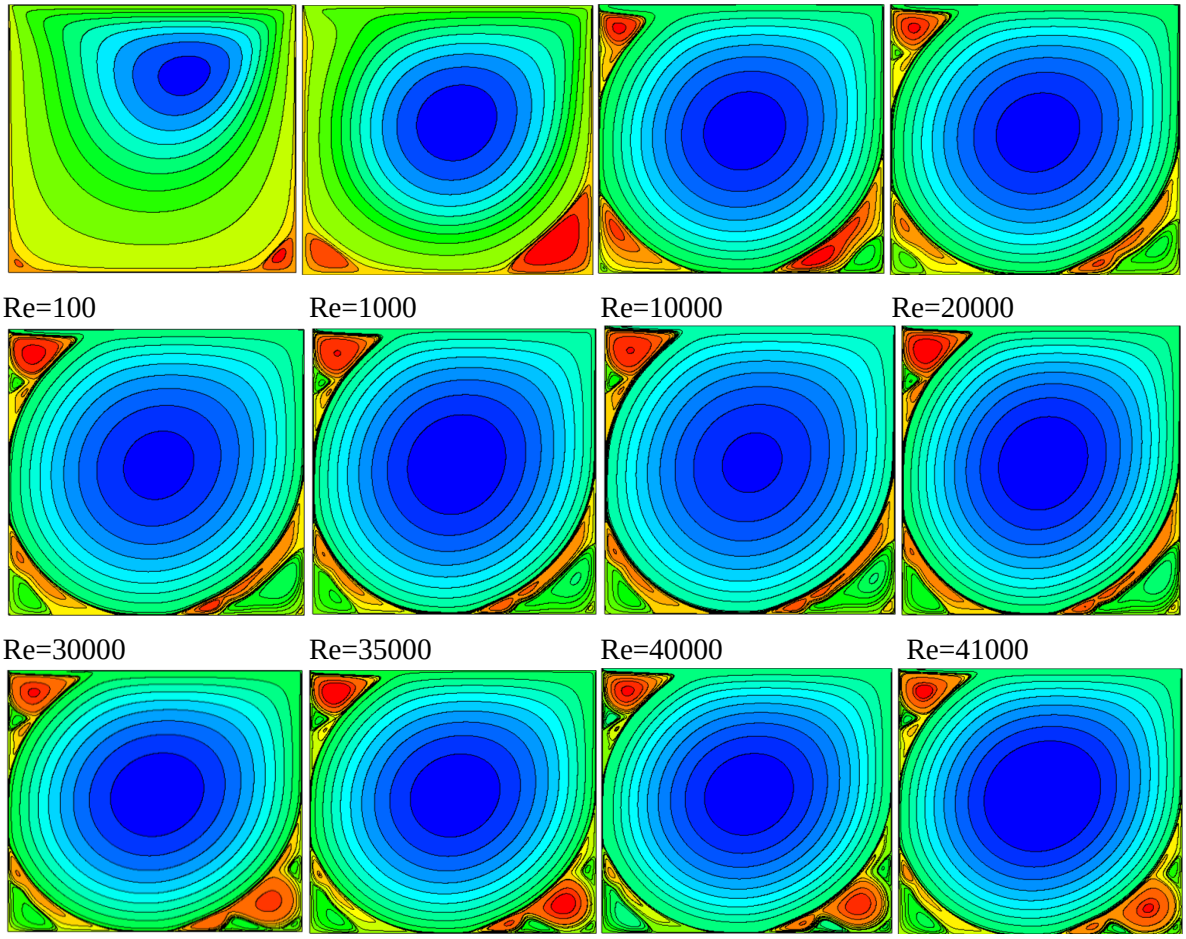

Figure 5 Stream function contours obtained at various Reynolds numbers.

to be verified through in-depth comparison represents in Fig 4 which shows a comparison of the horizontal velocities (u) along the vertical centerline (x=0.5) and the vertical velocities (v) along the horizontal centerline at (y=0.5) for Reynolds numbers in the range of $10000 \leq Re \leq 50000$ with multiple references. For Re=10000, solution data are compared with the results of Ghia et al [9] for 256×256 grid mesh and with Erturk [14] for 1024×1024 grid mesh while solution data for Re=20000 are compared only with Erturk [14]. also, for both Re=30000 and Re=35000, the comparison was carried out with numerical results of Wahba [16] for 501×501. otherwise the two profiles (u,v) for Re=40000, Re=45000 represent the current study, these results mentioned above revealed a great concurrence except for Re=50000 the unstable solution data of Hachem et al [15] for 180×180 are inconsistent with present results which confirming the effect of grid mesh on the stability of the numerical solutions.

Fig 5 shows the configuration of flow pattern in the cavity represented by stream function contours in steady state at various Reynolds numbers ranged for $100 \leq Re \leq 50000$. It is observed that the typical behavior of the flow configuration known by many authors in the literature agrees very well with that in this study for Re reached 41000. In addition to the primary vortex involved in the center of the domain a significant growth of the secondary vortices increases exponentially with increasing in the Reynolds numbers and affect the location centers of these vortices, the appearance of the third secondary vortices are very clear on the corners of the cavity.

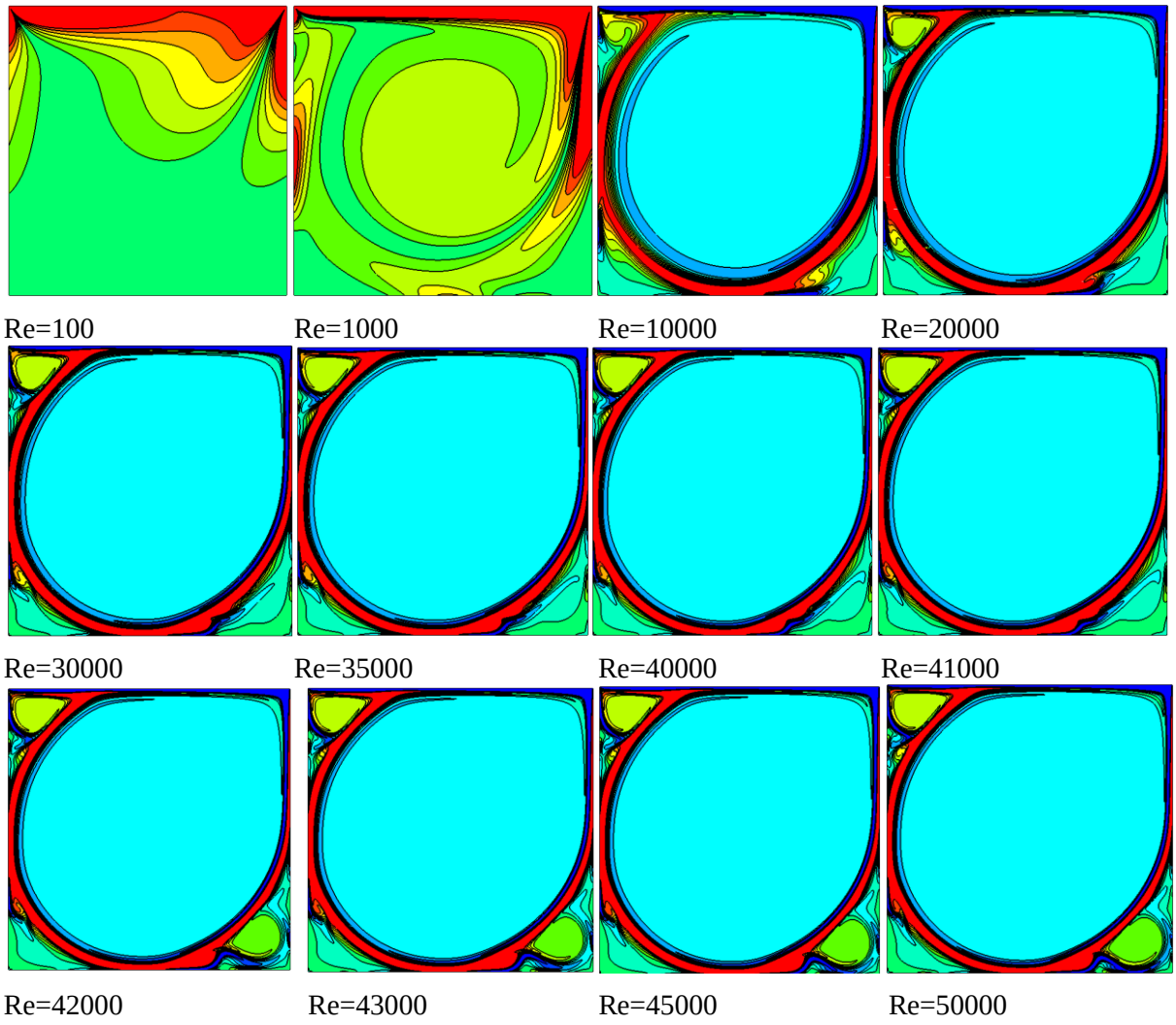

Figure 6 Vorticity contours obtained at various Reynolds numbers.

On the other hand, when Renolds number exceeds the threshold of 41000 especially within limits Re=41710, a very significant change in the flow pattern was observed at the bottom right of the domain of the cavity as an unexpected behavior represents by the appearance of five secondary vortices in different sizes while the first two counter-rotating secondary vortices consisting of one small vortex with small size neighboring by another with a large size which is also surrounded by three adjacent second secondary vortices have the same sense of rotation as the primary vortex, in which for the remaining two corners of the cavity(bottom left) and (top left), the flow pattern keeps up the same structure with a slightly change on the location of these secondary vortices.

Fig 6 presents the vorticity contours obtained at various Reynolds numbers. The regions indicated by concentration designate the high vorticity values localized there. Moreover, as shown in Tables 4-5, as Re increases as the strength of the secondary vortices increases with a slight drop in strength of the primary vortex which remains relatively constant.

Tables 4-5, show the properties of the flow for primary and secondary vortices for $100 \leq Re \leq 40000$, including values of stream function, vorticity, and location of the vortex, the names of the vortices are abbreviated as follow: PV, BR, BL, TL express either primary vortex, bottom right, bottom left, top left respectively whereas the numbers indicate the hierarchy of these secondary vortices 1, 2, and 3 expresses either first, second, and third respectively.

Table 4 Properties of primary and Bottom right secondary.

		Re						
		100	1000	10000	20000	30000	35000	40000
PV	ψ	-0.1035204	-0.118929	-0.122323	-0.12202	-0.121787	-0.121612	-0.121554
	ω	-3.16698	-2.0676	-1.91861	-1.903689	-1.89846	-1.895308	-1.895056
	(x, y)	(0.6157, 0.7373)	(0.5308, 0.5653)	(0.5118, 05300)	(0.5093, 0.5269)	(0.5081, 0.5257)	(0.5078, 0.5249)	(0.5073, 0.5247)
$BR1$	ψ	1.274E-05	1.73030E-03	3.1888E-03	2.79857E-03	2.96556E-03	2.34589E-03	2.23583E-03
	ω	3.524367E-02	1.107643	3.781775	6.216516	8.482063	9.54100	10.52671
	(x, y)	(0.9424, 0.0618)	(0.8640, 0,1117)	(0.7748, 0.0594)	(0.7213, 0.0431)	(0.6856, 0.0340)	(0.6722, 0.0311)	(0.6607, 0.0287)
$BR2$	ψ	-	-5.2E-8	-1.40964E-04	-4.63858E-04	-6.68679E-04	-7.493584E-04	-8.2407E-04
	ω	-	-7.911979E-03	-0.297161	-0.563582	-0.65354	-0.663195	-0.67165
	(x, y)	-	(0.9926, 0.0074)	(0.9349, 0.0679)	(0.9302, 0.1053)	(0.9319, 0.1218)	(0.9303, 0.1229)	(0.9278, 0.1224)
$BR3$	ψ	-	-	-	2.385E-08	4.36866-07	1.55514E-06	3.79972E-06
	ω	-	-	-	4.71657E-03	1.99580E-02	0.03898	0.064623
	(x, y)	-	-	-	(0.9939, 0.0070)	(0.9862, 0.0162)	(0.9815, 0.0214)	(0.9773, 0.0253)

The configuration of flow pattern in the cavity when the Reynolds numbers exceed the threshold Re=41710 are shown in Fig 8, the vortices' abbreviations names maintain the same as mentioned above except a simple addition of a tiny letter in order to signify the order of appearance of the secondary vortices in the bottom right of the cavity. While, the properties of the flow are tabulated in Table 6 for primary and secondary vortices for both Re=45000, Re=50000.

Tables 6-7 show the numerical values corresponding to u and v velocity passing through the vertical centerline and the horizontal centerline for $100 \leq Re \leq 50000$.

Table 5 Proprerties of Bottom left and Top left secondary vortices.

		Re						
		100	1000	10000	20000	30000	35000	40000
$BL1$	ψ	1.81E-06	2.33412E-04	1.6149E-03	1.630111E-03	1.50016E-03	1.44003E-03	1.37819E-03
	ω	1.50452E-02	0.351918	2.149298	2.957627	3.905502	4.364118	4.81725
	(x, y)	(0.0345, 0.0344)	(0.0832, 0.0780)	(0.0589, 0.1618)	(0.0480, 0.1830)	(0.0401, 0.2016)	(0.037, 0.2093)	(0.0345, 0.2162)
$BL2$	ψ	-	-8E-09	-1.1205E-06	-8.38227E-05	-1.806998E-04	-2.094140E-04	-2.33661E-04
	ω	-	-2.739669	-3.17418E-02	-0.252762	-0.368702	-0.407321	-0.443164
	(x, y)	-	(0.0048, 0.0048)	(0.0170, 0.0203)	(0.0590, 0.0544)	(0.0737, 0.0595)	(0.0790, 0.0579)	(0.0851, 0.0558)
$BL3$	ψ	-	-	-	2.15069E-09	7.96666E-09	1.359714E-08	1.1925E-08
	ω	-	-	-	1.7053507E-03	3.13831E-03	3.92891E-03	4.10412E-03
	(x, y)	-	-	-	(0.0034, 0.0031)	(0.0044, 0.0041)	(0.0049, 0.0049)	(0.0054, 0.0053)
$TL1$	ψ	-	-	2.631351E-03	3.76156E-03	4.39063E-03	4.63383E-03	4.841882E-03
	ω	-	-	2.311531	2.51234	2.63238	2.68339	2.721027
	(x, y)	-	-	(0.0704, 0.9112)	(0.0805, 0.9117)	(0.0848, 0.9128)	(0.0863, 0.9129)	(0.0875, 0.9131)
$TL2$	ψ	-	-	-	-7.336075E-05	-1.807805E-04	-2.19032E-04	-2.49953E-04
	ω	-	-	-	-0.975955	-1.35001	-1.43439	-1.540045
	(x, y)	-	-	-	(0.0247, 0.8192)	(0.0310, 0.8119)	(0.0313, 0.8093)	(0.0309, 0.8073)

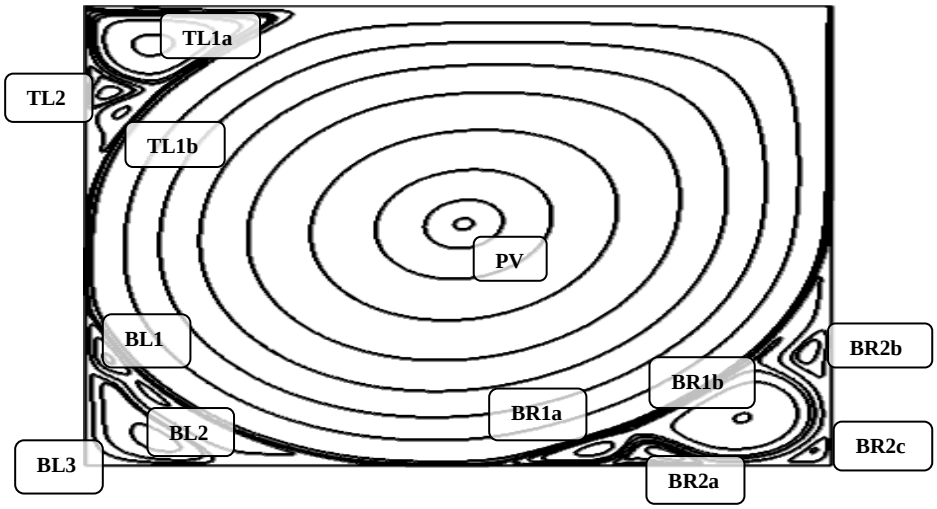

Figure 8 Flow configuration for Re ≥ 41710.

Table 6 Properties of primary and secondary vortices.

		Re				Re	
		45000	50000			45000	50000
Primary vortex	ψ	-0.121548	-0.121470	BL1	ψ	1.342516E-03	1.293551E-03
	ω	-1.894415	-1.893674		ω	5.364649	5.812606
	(x,y)	(0.5073, 0.5245)	(0.5070, 0.5241)		(x,y)	(0.0321, 0.2251)	(0.0302, 0.2304)
BR1a	ψ	3.006625E-03	2.91424E-03	BL2	ψ	-2.660884E-04	-2.90259E-04
	ω	8.3370	8.97085		ω	-0.476916	-0.497776
	(x,y)	(0.6943, 0.0369)	(0.6855, 0.0351)		(x,y)	(0.0914, 0.0547)	(0.0947, 0.0537)
				BL3	ψ	3.177777E-08	5.664E-08
BR1b	ψ	4.458081E-03	4.78432E-03		ω	5.679480E-03	7.89659E-03
	ω	1.756255	1.822144		(x,y)	(0.0071, 0.0064)	(0.0088, 0.0078)
	(x,y)	(0.8866, 0.1071)	(0.8817, 0.1031)				
				TL1a	ψ	5.004871E-03	5.16770E-03
BR2a	ψ	-3.284708E-04	-3.21092E-04		ω	2.758090	2.79116
	ω	-2.47146	-2.77719		(x,y)	(0.0884, 0.9133)	(0.0892, 0.9136)
	(x,y)	(0.7971, 0.0252)	(0.7802, 0.0230)				
				TL1b	ψ	7.302959E-4	8.10963E-04
					ω	3.613825	3.348625
BR2b	ψ	-8.58804E-05	-9.80703E-05		(x,y)	(0.0509, 0.7702)	(0.0460, 0.7655)
	ω	-6.26041E-01	-0.63670				
	(x,y)	(0.9704, 0.2440)	(0.9691, 0.2465)	TL2	ψ	-2.734150E-04	-2.97105E-04
					ω	-1.654226	-1.790126
BR3	ψ	-3.4603E-05	-6.593614E-05		(x,y)	(0.0299, 0.8077)	(0.0292, 0.8086)
	ω	-0.628747	-0.941995				
	(x,y)	(0.9794, 0.0254)	(0.9781, 0.0325)				

4 conclusion

Numerical study of two-dimensional (2D) incompressible steady flow in the lid-driven square cavity for 100≤Re≤50000, was carried out in the present paper. The finite volume method (FVM) and the COUPLED algorithm to treat pressure-velocity coupling with a very fine grid mesh used herein show great efficiency in terms of stabillity, robustness and accurracy for steady solutions at high Reynolds numbers. An eccentric behavior has been shown in flow structure for Re>41000, in the bottom right

Table 7 Values for u-velocity through the vertical centerline of the cavity.

y	Re								
	100	1000	10000	20000	30000	35000	40000	45000	50000
0.0000	0.00000	0.00000	0.00000	0.00000	0.00000	0.00000	0.00000	0.00000	0.00000
0.0100	-0.00745	-0.0398	-0.19054	-0.24281	-0.26713	-0.27522	-0.28192	-0.30442	-0.31143
0.0200	-0.01458	-0.07606	-0.2969	-0.36718	-0.40465	-0.41646	-0.42542	-0.44052	-0.44558
0.0301	-0.02142	-0.10923	-0.37849	-0.44549	-0.46098	-0.46108	-0.45932	-0.45755	-0.45382
0.0401	-0.02801	-0.13984	-0.43474	-0.46222	-0.45021	-0.44367	-0.43849	-0.43467	-0.43169
0.0501	-0.03437	-0.16852	-0.45754	-0.44539	-0.43026	-0.42652	-0.42444	-0.42338	-0.42236
0.0601	-0.04054	-0.1959	-0.45342	-0.42693	-0.41942	-0.41791	-0.41702	-0.41601	-0.41508
0.0701	-0.04652	-0.22241	-0.43695	-0.41519	-0.41159	-0.41029	-0.40939	-0.40793	-0.40701
0.0802	-0.05236	-0.24824	-0.41976	-0.40655	-0.40338	-0.40202	-0.40119	-0.39958	-0.3988
0.0902	-0.05806	-0.27328	-0.4062	-0.3981	-0.39479	-0.39355	-0.39287	-0.39123	-0.39057
0.1002	-0.06366	-0.29717	-0.39572	-0.38929	-0.38614	-0.38504	-0.38449	-0.38285	-0.38227
0.1723	-0.10197	-0.38853	-0.32989	-0.32469	-0.32291	-0.32224	-0.32201	-0.32075	-0.32044
0.2004	-0.11647	-0.37566	-0.30408	-0.29941	-0.29782	-0.2972	-0.29701	-0.29592	-0.29565
0.2826	-0.1583	-0.27889	-0.22854	-0.22473	-0.22341	-0.22288	-0.22269	-0.222	-0.22179
0.3006	-0.16708	-0.25847	-0.21195	-0.20825	-0.20696	-0.20644	-0.20625	-0.20562	-0.20542
0.4509	-0.21391	-0.11035	-0.07311	-0.06999	-0.06879	-0.06836	-0.0681	-0.06776	-0.06758
0.5010	-0.20891	-0.06107	-0.02629	-0.02331	-0.02212	-0.02172	-0.02143	-0.02113	-0.02095
0.6012	-0.15324	0.04028	0.06962	0.07225	0.07336	0.07366	0.07398	0.07424	0.07442
0.8016	0.11805	0.27423	0.28497	0.28516	0.28509	0.28484	0.28488	0.28497	0.28491
0.8517	0.23686	0.33732	0.34858	0.34753	0.34678	0.34625	0.34608	0.34605	0.34583
0.9018	0.41615	0.3857	0.4188	0.41637	0.41481	0.41396	0.41351	0.41333	0.41291
0.9319	0.5657	0.41332	0.46603	0.4617	0.45962	0.4586	0.458	0.45773	0.45719
0.9419	0.62298	0.43283	0.4817	0.47799	0.47537	0.47426	0.47361	0.47332	0.47276
0.9519	0.68361	0.46693	0.49454	0.49498	0.49193	0.49056	0.48974	0.48936	0.48874
0.9619	0.74709	0.52411	0.50077	0.51034	0.50932	0.50799	0.50699	0.50641	0.50558
0.9720	0.81275	0.61213	0.49632	0.51679	0.52268	0.5233	0.52356	0.52375	0.52334
0.9820	0.8797	0.73321	0.49759	0.50369	0.51638	0.52066	0.52425	0.52743	0.52957
0.9920	0.94689	0.87899	0.65569	0.56525	0.52571	0.51514	0.50852	0.50499	0.50277
1.0000	1.00000	1.00000	1.00000	1.00000	1.00000	1.00000	1.00000	1.00000	1.00000

Table 8 Values for v-velocity through the vertical centerline of the cavity.

x	Re								
	100	1000	10000	20000	30000	35000	40000	45000	50000
0.0000	0.00000	0.00000	0.00000	0.00000	0.00000	0.00000	0.00000	0.00000	0.00000
0.0100	0.01832	0.07103	0.21325	0.27495	0.3114	0.32462	0.33603	0.34572	0.35432
0.0200	0.0354	0.13081	0.33013	0.39103	0.42578	0.438112	0.44851	0.45668	0.4637
0.0301	0.05128	0.17984	0.39323	0.45218	0.47633	0.4818	0.48509	0.48634	0.48685
0.0401	0.06598	0.21919	0.43595	0.476	0.48015	0.47847	0.47651	0.47418	0.47232
0.0501	0.07954	0.25044	0.45918	0.47234	0.46553	0.46252	0.46054	0.45878	0.45768
0.0601	0.092	0.27546	0.46448	0.45812	0.45082	0.44883	0.44768	0.44647	0.44566
0.0701	0.10341	0.29595	0.45756	0.4436	0.4385	0.43694	0.43592	0.43475	0.4339
0.0802	0.11381	0.31322	0.44484	0.43101	0.42691	0.42533	0.42429	0.42314	0.42231
0.0902	0.12324	0.32813	0.43088	0.41944	0.41544	0.41386	0.41284	0.41176	0.41097
0.1002	0.13177	0.34107	0.41772	0.40813	0.40412	0.40258	0.4016	0.40059	0.39983
0.1723	0.17039	0.37467	0.3376	0.33014	0.32688	0.32562	0.32486	0.32424	0.32363
0.2004	0.17678	0.35886	0.30795	0.30111	0.29811	0.29693	0.29623	0.29573	0.29517
0.2826	0.17567	0.26728	0.22355	0.21825	0.21588	0.21493	0.21437	0.21412	0.21365
0.3006	0.17209	0.24541	0.20537	0.20036	0.19811	0.19721	0.19666	0.19645	0.19601
0.4509	0.09901	0.07856	0.05672	0.05374	0.05228	0.05172	0.05131	0.05126	0.05093
0.5010	0.0566	0.02471	0.0077	0.00533	0.0041	0.00366	0.00329	0.00325	0.00296
0.6012	-0.05409	-0.08433	-0.0912	-0.09225	-0.09291	-0.09309	-0.09336	-0.0934	-0.0936
0.8016	-0.25318	-0.31593	-0.30308	-0.30015	-0.29892	-0.29834	-0.29813	-0.29807	-0.29788
0.8517	-0.23957	-0.40725	-0.36132	-0.35687	-0.35484	-0.35397	-0.35353	-0.35338	-0.35301
0.9018	-0.18391	-0.52312	-0.42245	-0.41586	-0.41275	-0.41148	-0.41072	-0.4104	-0.40978
0.9319	-0.13372	-0.48226	-0.45492	-0.45221	-0.44839	-0.44671	-0.4456	-0.4451	-0.44426
0.9419	-0.11505	-0.43153	-0.46948	-0.46251	-0.4602	-0.4586	-0.4574	-0.4568	-0.45582
0.9519	-0.09572	-0.36411	-0.50245	-0.47112	-0.46989	-0.46917	-0.46852	-0.46824	-0.46735
0.9619	-0.07593	-0.28513	-0.55857	-0.49362	-0.47802	-0.47619	-0.47575	-0.47623	-0.47608
0.9720	-0.05588	-0.2015	-0.57383	-0.5603	-0.52092	-0.50712	-0.49742	-0.49109	-0.4866
0.9820	-0.03576	-0.12049	-0.42766	-0.53668	-0.5713	-0.57543	-0.57543	-0.57334	-0.56929
0.9920	-0.01577	-0.04837	-0.15418	-0.20533	-0.23808	-0.25025	-0.26051	-0.2724	-0.27938
1.0000	1.00000	1.00000	0.00000	0.00000	0.00000	0.00000	0.00000	0.00000	0.00000

of the cavity. Properties of flow were tabulated for a wide field and a good agreement are found in the literature, and new numerical results for 35000<Re≤50000 was displayed. Values of velocity profiles are provided For benchmarking purposes. Finally, although that the present study interested in the steady form of Navier-Stokes to reach steady solutions, it is recommended to further investigations in an unsteady form based on turbulence models for the sake of comparison.

Nomenclature

p pressure	ω vorticity
u velocity component on x	x horizontal coordinate
v velocity component on y	y vertical coordinate
V velocity vector	L length (physical size of the cavity)
μ dynamic viscosity	CFL flow courant number
ρ density	α under-relaxation factor
ψ stream function	Re Reynolds number

References

[1] O.R. Burggraf, Analytical and numerical studies of the structure of steady separated flows, J. Fluid Mech. 24 (1966) 113–151.
[2] O. Botella, R. Peyret, Benchmark spectral results on the liddriven cavity flow, Comput. Fluids 27 (1998) 421–433.
[3] C.H. Marchi, R. Suero, L.K. Araki, The Lid-Driven Square Cavity Flow: Numerical Solution with a 1024 x 1024 Grid, J. Braz. Soc. Mech. Sci. & Eng. 31 (2009) 186-198.
[4] S.P. Vanka, Block-implicit multigrid solution of Navier-Stokes equations in primitive variables, J. Comput. Phys. 65 (1986) 138–158.
[5] T.A. AbelMigid, K.M. Saqr, M.A. Kotb, A.A. Aboelfarag, Revisiting the lid-driven cavity flow problem: Review and new steady state benchmarking results using GPU accelerated code, J. Alexandria Eng. 56 (2016) 123-135.
[6] C.H. Bruneau, C. Jouron, An efficient scheme for solving steady incompressible Navier-Stokes equations, J. Comput. Phys. 89 (1990) 389–413.
[7] S. Hou, Q. Zou, S. Chen, G. Doolen, A.C. Cogley, Simulation of cavity flow by the lattice Boltzmann method, J. Comput. Phys. 118 (1995) 329–347.
[8] J. Zhang, Numerical simulation of 2D square driven cavity using fourth-order compact finite difference schemes, J. Comput.Maths with Applications, 45 (2003) 43-52.
[9] U. Ghia, K.N. Ghia, C. Shin, High-Re solutions for incompressible flow using the Navier-Stokes equations and a multigrid method, J. Comput. Phys. 48 (1982) 387–411.
[10] R. Schreiber, H. Keller, Driven cavity flows by efficient numerical techniques, J. Comput. Phys. 49 (1983) 310–333.
[11] M.M. Gupta, J.C. Kalita, A new paradigm for solving NavierStokes equations: streamfunction–velocity formulation, J. Comput. Phys. 207 (2005) 52–68.
[12] E. Barragy, G. Carey, Stream function-vorticity driven cavity solution using p finite elements, J.Comput. Fluids 26 (1997) 453– 468.

[13] E. Erturk, T.C. Corke, C. Go¨kc¸o¨l, Numerical solutions of 2-D steady incompressible driven cavity flow at high Reynolds numbers, Int. J. Numer. Meth. Fluids 48 (2005) 747–774.
[14] E. Erturk, Discussions on driven cavity flow, Int. J. Numer. Meth. Fluids 60 (2009) 275–94.
[15] E. Hachem, B.Rivaux, T.Kloczko, H.Digonnet, T.Coupez, Stabilized finite element method for incompressible flows with high Reynolds number, J. Comput. Phys 229 (2010) 8643-8665.
[16] E.M.Wahba, Steady flow simulations inside a driven cavity up to Reynolds number 35000, J. Comput. Fluids 66 (2012) 85–97.
[17] Y.H. Peng, Y.H. Shiau, R.R. Hwang, Transition in a 2-D lid-driven cavity flow, J. Comput. Fluids 32 (2003) 337-352.
[18] F. Auteri, N. Parolini, L. Quartapelle, Numerical investigation on the stability of singular driven cavity flow, J. Comput. Phys 183 (2002) 1-25.
[19] A. Fortin, M.Jardak, JJ.Gervais, R.Pierre, Localization of Hopf bifurcations in fluid flow problems, International Journal for Numerical Methods in Fluids 24 (1997) 1185-1210.
[20] M. Sahin, R.G.Owens, A novel fully-implicit finite volume method applied to the lid-driven cavity flow problem, Part II, Linear stability analysis, International Journal for Numerical Methods in Fluids 42 (2003) 79-88.
[21] A. Abouhamza, R.Pierre, A neutral stability curve for incompressible flows in a rectangular driven cavity, Mathematical and Computer Modelling 38 (2003) 141-157.
[22] J.J. Gervais, D. Lemelin, R. Pierre, Some experiments with stability analysis of discrete incompressible flows in the lid-driven cavity, International Journal for Numerical Methods in Fluids 24 (1997) 477-492.
[23] C.-H. Bruneau, M. Saad, The 2D lid-driven cavity problem revisited, Comput. Fluids 35 (2006) 326–348.
[24]] J.H. Ferziger, M. Peric´, Computational Methods for Fluid Dynamics, third, rev. ed., Springer, Berlin; New York, 2002.